Journal of Medicinal Chemistry Article

J. Med. Chem. **2010,** *53,* 2843–2853 **2843**
DOI: 10.1021/jm9018146

The Impact of Polyether Chain Length on the Iron Clearing Efficiency and Physiochemical Properties of Desferrithiocin Analogues

Raymond J. Bergeron,*[,†] Neelam Bharti,[†] Jan Wiegand,[†] James S. McManis,[†] Shailendra Singh,[†] and Khalil A. Abboud[‡]

[†]*Department of Medicinal Chemistry University of Florida, Gainesville, Florida 32610-0485, and* [‡]*Department of Chemistry, University of Florida, Gainesville, Florida 32611*

Received December 8, 2009

(*S*)-2-(2,4-Dihydroxyphenyl)-4,5-dihydro-4-methyl-4-thiazolecarboxylic acid (**2**) was abandoned in clinical trials as an iron chelator for the treatment of iron overload disease because of its nephrotoxicity. However, subsequent investigations revealed that replacing the 4′-(HO) of **2** with a 3,6,9-trioxadecyloxy group, ligand **4**, increased iron clearing efficiency (ICE) and ameliorated the renal toxicity of **2**. This compelled a closer look at additional polyether analogues, the subject of this work. The 3,6,9,12-tetraoxatridecyloxy analogue of **4**, chelator **5**, an oil, had twice the ICE in rodents of **4**, although its ICE in primates was reduced relative to **4**. The corresponding 3,6-dioxaheptyloxy analogue of **2**, **6** (a crystalline solid), had high ICEs in both the rodent and primate models. It significantly decorporated hepatic, renal, and cardiac iron, with no obvious histopathologies. These findings suggest that polyether chain length has a profound effect on ICE, tissue iron decorporation, and ligand physiochemical properties.

Introduction

In humans with iron overload disease, the toxicity associated with an excess of this metal derives from iron's interaction with reactive oxygen species, for instance, endogenous hydrogen peroxide (H_2O_2).[1−4] In the presence of Fe(II), H_2O_2 is reduced to the hydroxyl radical ($HO^•$), a very reactive species, and HO^-, the Fenton reaction. The hydroxyl radical reacts very quickly with a variety of cellular constituents and can initiate free radicals and radical-mediated chain processes that damage DNA and membranes as well as produce carcinogens.[2,5,6] The Fe(III) liberated can be reduced back to Fe(II) via a variety of biological reductants (e.g., ascorbate, glutathione), a problematic cycle.

The iron-mediated damage can be focal, as in reperfusion damage,[7] Parkinson's,[8] and Friedreich's ataxia,[9] or global, as in transfusional iron overload, e.g., thalassemia,[10] sickle cell disease,[10,11] and myelodysplasia,[12] with multiple organ involvment. The solution in both scenarios is the same: chelate and promote the excretion of excess unmanaged iron. The design, synthesis, and evaluation of ligands for the treatment of transfusional iron overload diseases represent the focus of the current study.

While humans have a highly efficient iron management system in which they absorb and excrete about 1 mg of iron daily, there is no conduit for the excretion of excess metal. Transfusion-dependent anemias, like thalassemia, lead to a build up of iron in the liver, heart, pancreas, and elsewhere, resulting in (i) liver disease that may progress to cirrhosis,[13−15] (ii) diabetes related both to iron-induced decreases in pancreatic β-cell secretion and to increases in hepatic insulin resistance,[16,17] and (iii) heart disease. Cardiac failure is still the leading cause of death in thalassemia major and related forms of transfusional iron overload.[18−20]

Treatment with a chelating agent capable of sequestering iron and permitting its excretion from the body is the only therapeutic approach available. Some of the iron-chelating agents that are now in use or that have been clinically evaluated include desferrioxamine B mesylate (DFO[a]),[21] 1,2-dimethyl-3-hydroxy-4-pyridinone (deferiprone, L1),[22−25] 4-[3,5-bis(2-hydroxyphenyl)-1,2,4-triazol-1-yl]benzoic acid (deferasirox, ICL670A),[26−29] and the desferrithiocin, (*S*)-4,5-dihydro-2-(3-hydroxy-2-pyridinyl)-4-methyl-4-thiazolecarboxylic acid (DFT, **1**, Table 1), analogue, (*S*)-2-(2,4-dihydroxyphenyl)-4,5-dihydro-4-methyl-4-thiazolecarboxylic acid [deferitrin (**2**),[30] Table 1]. Each of these ligands presents with serious shortcomings. DFO must be given subcutaneously for protracted periods of time, e.g., 12 h a day, five days a week, a serious patient compliance issue.[31−33] Deferiprone, while orally active, simply does not remove enough iron to maintain patients in a negative iron balance.[22−25] Deferasirox did not show noninferiority to DFO and is associated with numerous side effects; it has a very narrow therapeutic window.[26−29] Finally, the clinical trial on **2** (Table 1) was abandoned by Genzyme because of renal toxicity.[30] However, deferitrin (**2**) has been reengineered, leading to the discovery that replacing the 4′-hydroxyl on the aromatic ring of **2** with a 3,6,9-trioxadecyloxy polyether group solved the renal toxicity issue;[34] iron clearing efficiency (ICE) was also improved. These findings drive the current study, which focuses on the impact of polyether chain length on ligand iron clearing efficiency and toxicity. The ultimate goal is to identify a chelator that is orally active in an

*To whom correspondence should be addressed. Phone: (352) 273-7725. Fax: (352) 392-8406. E-mail: rayb@ufl.edu. Address: Box 100485 JHMHSC, Department of Medicinal Chemistry, University of Florida, Gainesville, Florida 32610-0485.

[a] Abbreviations: dec, decomposes; DFO, desferrioxamine B mesylate; DFT, desferrithiocin [(*S*)-4,5-dihydro-2-(3-hydroxy-2-pyridinyl)-4-methyl-4-thiazolecarboxylic acid]; DIEA, *N*,*N*-diisopropylethylamine; DMF, *N*,*N*-dimethylformamide; DMSO, dimethyl sulfoxide; ICE, iron-clearing efficiency; log P_{app}, octanol−water partition coefficient (lipophilicity); MIC, maximum iron clearance.

Published on Web 03/16/2010

Table 1. Iron-Clearing Efficiency of Desferrithiocin Analogues Administered Orally to Rodents and Primates with the Respective Log P_{app} Values and Physiochemical Properties

Chelator/ Compound Number	[a]Rodent Iron-Clearing Efficiency (%)	[c]Primate Iron-Clearing Efficiency (%)	[f]Performance Ratio	[g]Log P_{app}	Physical State/ [h]Melting Point
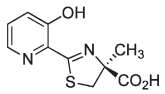 **1**	5.5 ± 3.2 [93/7]	16.1 ± 8.5 [78/22]	2.9	-1.77	solid mp 154 °C (dec)
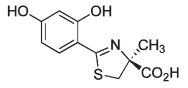 **2**	1.1 ± 0.8 [100/0]	16.8 ± 7.2 [88/12]	15.3	-1.05	solid mp 281 - 283 °C (dec)
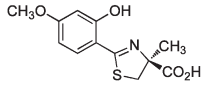 **3**	6.6 ± 2.8 [98/2]	24.4 ± 10.8 [91/9]	3.7	-0.70	solid mp 77 – 79 °C
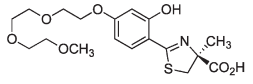 **4**	5.5 ± 1.9 [90/10]	25.4 ± 7.4 [96/4]	4.6	-1.10	oil
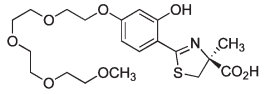 **5**	12.0 ± 1.5 [99/1]	9.8 ± 1.9 [52/48]	0.8	-1.23	oil
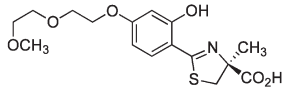 **6**	26.7 ± 4.7[b] [97/3]	26.3 ± 9.9[d] [93/7] 28.7 ± 12.4[e] [83/17]	1.0 1.1	-0.89	solid mp 82-83 °C
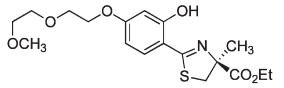 **7**	25.9 ± 6.5[b] [99/1]	8.8 ± 2.2 [98/2]	0.3	3.00	solid mp 68-70 °C

[a] In the rodents [n = 3 (**6**), 4 (**3**–**5**, **7**), 5 (**1**), 8 (**2**)], the drugs were given po at a dose of 150 μmol/kg (**1**) or 300 μmol/kg (**2**–**7**). The drugs were administered in capsules (**6**, **7**), solubilized in either 40% Cremophor RH-40/water (**1**), distilled water (**4**), or were given as their monosodium salts, prepared by the addition of 1 equiv of NaOH to a suspension of the free acid in distilled water (**2**, **3**, **5**). The efficiency of each compound was calculated by subtracting the 24 h iron excretion of control animals from the iron excretion of the treated animals. The number was then divided by the theoretical output; the result is expressed as a percent. The ICE data for ligand **1** is from ref 39. The ICE data for **2**–**4** are from ref 34. [b] ICE is based on a 48 h sample collection period. The relative percentages of the iron excreted in the bile and urine are in brackets. [c] In the primates [n = 4 (**1**, **3**, **4**, **5**, **6** in capsules, **7**) or 7 (**2**, **6** as the monosodium salt)], the chelators were given po at a dose of 75 μmol/kg (**5**–**7**) or 150 μmol/kg (**1**–**4**). The drugs were administered in capsules (**6**[d], **7**), solubilized in either 40% Cremophor RH-40/water (**1**, **3**), distilled water (**4**), or were given as their monosodium salts, prepared by the addition of 1 equiv of NaOH to a suspension of the free acid in distilled water (**2**, **5**, **6**[e]). The efficiency was calculated by averaging the iron output for 4 days before the drug, subtracting these numbers from the 2 day iron clearance after the administration of the drug, and then dividing by the theoretical output; the result is expressed as a percent. The ICE data for ligand **1** is from refs 40, 41. The ICE data for **2**–**4** are from refs 42, 43, and 34, respectively. The relative percentages of the iron excreted in the feces and urine are in brackets. [f] Performance ratio is defined as the mean $ICE_{primates}/ICE_{rodents}$. [g] Data are expressed as the log of the fraction in the octanol layer (log P_{app}); measurements were done in TRIS buffer, pH 7.4, using a "shake flask" direct method.[52] The values for **2** and **3** are from ref 43; the value for **4** is from ref 34. [h] The mp data for **1**–**3** are from ref 39, 42, and 43, respectively.

acceptable dosage form, is very efficient at decorporating iron, and has a broad therapeutic window. The boundary condition set by many hematologists is that the chelator should be able to remove 450 μg/kg/day of the metal.[35]

Results and Discussion

Design Concept. DFT (**1**) is a natural product iron chelator, a siderophore. It forms a tight 2:1 complex with Fe(III), has a log β_2 of 29.6,[36–38] and was one of the first iron chelators shown to be orally active. It performed well in both the bile duct-cannulated rodent model (ICE, 5.5%)[39] and in the iron-overloaded *Cebus apella* primate (ICE, 16%).[40,41] Unfortunately, **1** was severely nephrotoxic.[41] Nevertheless, its outstanding oral activity spurred a structure–activity study to identify an orally active and safe DFT analogue. The first goal was to define the minimal structural platform, pharmacophore, compatible with iron clearance upon oral administration.[42–44]

Removal of the pyridine nitrogen of DFT provided (*S*)-4,5-dihydro-2-(2-hydroxyphenyl)-4-methyl-4-thiazolecarboxylic acid [(*S*)-DADFT],[44] the parent ligand of the desaza (DA) series. Substitution of the 4-methyl of (*S*)-DADFT with a hydrogen led to (*S*)-4,5-dihydro-2-(2-hydroxyphenyl)-4-thiazolecarboxylic acid [(*S*)-DADMDFT],[41,44] the platform for the ensuing DADM systems. In the course of additional structure−activity relationship (SAR) studies, we were able to determine that within a given family of ligands, e.g., the DADFTs or the DADMDFTs, that the chelator's log P_{app}, lipophilicity, had a profound effect on both ICE and toxicity.[34,43,45] In each family, as the lipophilicity decreases, i.e., the log P_{app} becomes more negative, the toxicity also decreases. The more lipophilic chelators generally had greater ICE and increased toxicity.[34,43,45] It is critical to remain within families when making these comparisons. For example, there is no relationship between the log P_{app}, ICE, and toxicity of DFT itself versus the log P_{app}, ICE, and toxicity of its analogues. However, in the case of the desaza family of ligands, for example, when a 4′-(CH_3O) group was fixed in place of the 4′-(HO) of **2**, providing (*S*)-4,5-dihydro-2-(2-hydroxy-4-methoxyphenyl)-4-methyl-4-thiazolecarboxylic acid (**3**, Table 1), the molecule's lipophilicity increased, as did its ICE and toxicity.[34,43] This ligand is very lipophilic, log $P_{app} = -0.70$, and a very effective iron chelator when given orally to rodents[34] or primates[43] (Table 1). Unfortunately, the ligand was also very nephrotoxic.[34] The question then became how to balance the lipophilicity/toxicity interaction while iron-clearing efficiency is maintained.

Scheme 1. Synthesis of (*S*)-4,5-Dihydro-2-[2-hydroxy-4-(3,6,9,12-tetraoxatridecyloxy)phenyl]-4-methyl-4-thiazolecarboxylic Acid (**5**)[a]

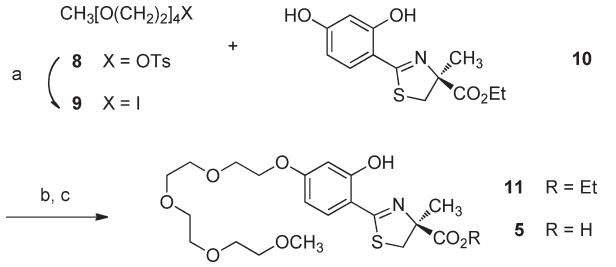

[a] Reagents and conditions: (a) NaI (2 equiv), acetone, reflux, 18 h, 94%; (b) **9** (1.3 equiv), K_2CO_3 (1.3 equiv), acetone, reflux, 2 d, 73%; (c) 50% NaOH (aq) (11 equiv), CH_3OH, 94%.

Ultimately, we discovered that fixing a polyether moiety, a 3,6,9-trioxadecyloxy group, to the 4′-position of **2**, providing (*S*)-4,5-dihydro-2-[2-hydroxy-4-(3,6,9-trioxadecyloxy)phenyl]-4-methyl-4-thiazolecarboxylic acid (**4**, Table 1), resulted in a ligand that retained the ICE properties of **3** but was much less lipophilic and less toxic than **3**.[34] This polyether fragment has been fixed to one of three positions on the aromatic ring, 3′-, 4′-, or 5′-.[34,46] The iron-clearing efficiency in rodents and primates is shown to be very sensitive to which positional isomer is evaluated.[34,46] In rodents, the polyethers had uniformly higher ICEs than their corresponding parent ligands. There was also a profound reduction in toxicity, particularly renal toxicity.[34,46,47] In the primate model, the ICEs for both the 3′- and 4′- polyethers were similar to the corresponding phenolic parent, e.g., the 3′-(HO) isomer of deferitrin (**2**) and **2**, respectively.[46] However, the ICE of the 5′-polyether substituted ligand decreased relative to its parent.[46] What remained unclear was the quantitative significance of the *length* of the polyether backbone on the properties of the ligands, the subject of this work.

In the current study, additional polyether analogues of **2** were synthesized (Table 1). Specifically, the 3,6,9-trioxadecyloxy substituent at the 4′-position of ligand **4** was both lengthened to provide (*S*)-4,5-dihydro-2-[2-hydroxy-4-(3,6,9,12-tetraoxatridecyloxy)phenyl]-4-methyl-4-thiazolecarboxylic acid (**5**) and shortened to provide (*S*)-4,5-dihydro-2-[2-hydroxy-4-(3,6-dioxaheptyloxy)phenyl]-4-methyl-4-thiazolecarboxylic acid (**6**). The ethyl ester of **6**, ethyl (*S*)-4,5-dihydro-2-[2-hydroxy-4-(3,6-dioxaheptyloxy)phenyl]-4-methyl-4-thiazolecarboxylate (**7**), was also prepared. Three questions were addressed regarding the structural changes in ligand **2**: (1) the effect on lipophilicity, (2) the effect on the iron clearing efficiency in the bile duct-cannulated rodent and primate models, and (3) the effect on the physiochemical properties of the ligand. We have consistently seen that, within a given family, ligands with greater lipophilicity are more efficient iron chelators, but are also more toxic,[34,43,45] thus issues 1 and 2. We have also observed that the polyether acids for the 3′- and 4′-3,6,9-trioxadecyloxy analogues are oils, and in most cases, the salts are hygroscopic. A crystalline solid ligand would offer greater flexibility in dosage forms.

Synthesis. Deferitrin (**2**) was converted to ethyl (*S*)-2-(2,4-dihydroxyphenyl)-4,5-dihydro-4-methyl-4-thiazolecarboxylate (**10**)[48] in this laboratory. With the carboxylate group protected as an ester, alkylation of the less sterically hindered 4′-hydroxy of **10** in the presence of the 2′-hydroxy, an iron

Scheme 2. Synthesis of (*S*)-4,5-Dihydro-2-[2-hydroxy-4-(3,6-dioxaheptyloxy)phenyl]-4-methyl-4-thiazolecarboxylic Acid (**6**) and Its Ethyl (**7**) and Isopropyl (**13**) Esters[a]

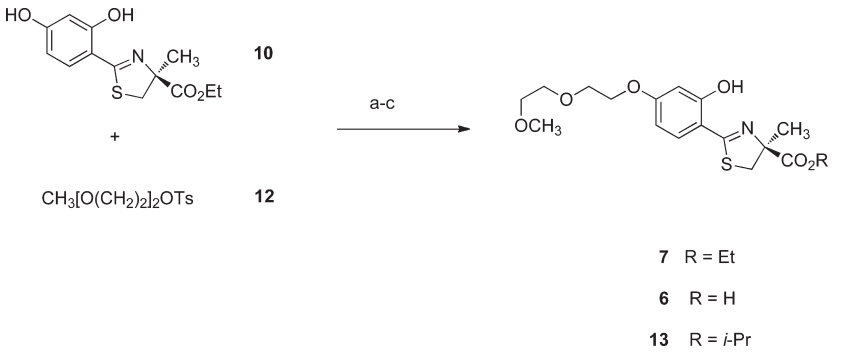

[a] Reagents and conditions: (a) K_2CO_3 (1.1 equiv), acetone, reflux, 2 d, 73%; (c) 50% NaOH (aq) (13 equiv), CH_3OH, 80%; (c) 2-iodopropane (1.6 equiv), DIEA (1.6 equiv), DMF, 3 d, 85%.

chelating site, has generated numerous desferrithiocin analogues, including **3**−**6** (Table 1).[34,43]

Thus, *O*-monoalkylation of ethyl ester **10** with 13-iodo-2,5,8,11-tetraoxatridecane (**9**) using potassium carbonate in refluxing acetone generated masked chelator **11** in 73% yield (Scheme 1). Tetraether iodide **9** was readily accessed in 94% yield from tosylate **8**,[49,50] employing sodium iodide (2 equiv) in refluxing acetone, as alkylating agent **8** possesses similar chromatographic properties to ester **11**. Hydrolysis of the ester protecting group of **11** in base completed the synthesis of 3,6,9,12-tetraoxatridecyloxy ligand **5**, a homologue of **4**[47] with an additional ethyleneoxy unit in the polyether chain, in 94% yield.

The synthesis of the 3,6-dioxaheptyloxy ligand (**6**), the analogue of chelator **4** with one less ethyleneoxy unit in the polyether chain, was prepared using similar strategy (Scheme 2). 4′-*O*-Alkylation of ethyl ester **10** with 3,6-dioxaheptyl 4-toluenesulfonate (**12**)[49] generated **7** in 73% *recrystallized* yield. Unmasking the carboxylate of **7** under alkaline conditions furnished the shorter 4′-polyether-derived iron chelator **6** in 80% *recrystallized* yield. Both ligand **6** and its ethyl ester **7** are crystalline solids and thus offer clear advantages both in large scale synthesis and in dosage forms over previously reported polyether-substituted DFTs, which are oils.[34,46,47] Carboxylic acid **6** was esterified using 2-iodopropane and *N*,*N*-diisopropylethylamine (DIEA) (1.6 equiv each) in DMF, providing isopropyl (*S*)-4,5-dihydro-2-[2-hydroxy-4-(3,6-dioxaheptyloxy)phenyl]-4-methyl-4-thiazolecarboxylate (**13**) in 85% yield as an oil (Scheme 2). This is consistent with the idea that the structural boundary conditions for ligand crystallinity are very narrow.

Physiochemical Properties. Single crystal X-ray analysis confirmed that chelator **6** (Figure 1) and its ethyl ester **7** (Figure 2) exist in the (*S*)-configuration. Both **6** and **7** crystallize in monoclinic lattices, space group $P2_1$, with two molecules in unit cell. Moreover, acid **6** has unit cell dimensions of a = 5.5157(5) Å, b = 8.8988(8) Å, and c = 17.3671(16) Å with α and γ = 90° and β = 98.322(1)°. The unit cell dimensions of ester **7** are a = 7.7798(6) Å, b = 8.9780(6) Å, and c = 14.1119(10) Å, also with α and γ = 90° but β = 106.078(1)°. Unit cell volumes (Å^3) of **6** and **7** are 843.46(13) and 947.12(12), respectively. In the crystal lattice of **6**, the acidic hydrogen is bonded to O6A of the carboxylate group, resulting in a neutral molecule (Figure 1). However, parent ligand **2** (Table 1) with a strongly electron donating 4′-hydroxy is zwitterionic, that is, an iminium ion is observed by X-ray crystallography.[51] Thus, not unexpectedly, deferitrin (**2**) (log P_{app} = −1.05) is more hydrophilic than polyether chelator **6** (log P_{app} = −0.89).

Partition Properties. The partition values between octanol and water (at pH 7.4, Tris buffer) were determined using a "shake flask" direct method of measuring log P_{app} values.[52] The fraction of drug in the octanol is then expressed as log P_{app}. These values varied widely (Table 1), from log P_{app} = −1.77 for **1** to log P_{app} = 3.00 for **7**. This represents a greater than 58000-fold difference in partition. The most lipophilic chelator, **7**, is 11220 times more lipophilic than the parent **2**.

Animal Models. There are no dependable in vitro assays for predicting the in vivo efficacy of an iron decorporation agent.[53,54] While tight iron binding is a necessary requirement for an effective iron chelator, it is not sufficient.[55] Once having established that a ligand platform, pharmacophore, binds iron tightly, e.g., desferrithiocin,[37,38] SAR studies

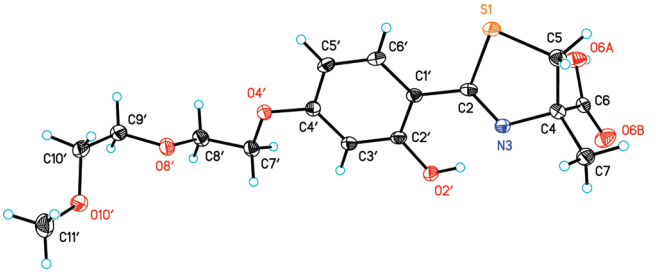

Figure 1. X-ray of (*S*)-4,5-dihydro-2-[2-hydroxy-4-(3,6-dioxaheptyloxy)phenyl]-4-methyl-4-thiazolecarboxylic acid (**6**). Structure is drawn at 50% probability ellipsoids.

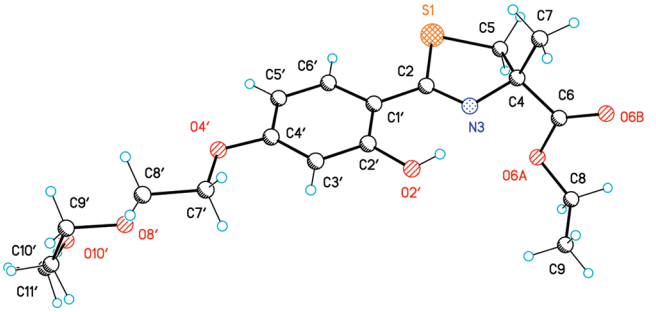

Figure 2. X-ray of ethyl (*S*)-4,5-dihydro-2-[2-hydroxy-4-(3,6-dioxaheptyloxy)phenyl]-4-methyl-4-thiazolecarboxylate (**7**). Structure is drawn at 50% probability ellipsoids.

focused on minimizing toxicity while optimizing iron clearance are carried out.

Chelator-Induced Iron Clearance in Non-Iron-Overloaded, Bile Duct-Cannulated Rodents. In the text below, "iron-clearing efficiency" (ICE) is used as a measure of the amount of iron excretion induced by a chelator. The ICE, expressed as a percent, is calculated as (ligand-induced iron excretion/theoretical iron excretion) × 100. To illustrate, the theoretical iron excretion after administration of one millimole of DFO, a hexadentate chelator that forms a 1:1 complex with Fe(III), is one milli-g-atom of iron. Two millimoles of desferrithiocin (DFT, **1**, Table 1), a tridentate chelator which forms a 2:1 complex with Fe(III), are required for the theoretical excretion of one milli-g-atom of iron. In the rodents, in each instance, the polyether analogues are better iron clearing agents than their phenolic counterparts, e.g., **2** vs **4**, **5**, **6**, or **7** (Table 1). We have included historical data (compounds **1**−**4**)[34,39,43] for comparative purposes. The ICE of the 3,6,9-trioxadecyloxy analogue (**4**) is five times greater than that of the parent ligand (**2**), 5.5 ± 1.9% vs 1.1 ± 0.8% (p < 0.003), respectively.[34] The longer ether analogue, 3,6,9,12-tetraoxatridecyloxy analogue (**5**), is nearly 11 times as efficient as **2**, with an ICE of 12.0 ± 1.5% (p < 0.001). The shorter ether analogue, the 3,6-dioxaheptoxy ligand (**6**), and its corresponding ethyl ester (**7**), are highly crystalline solids that were administered to the rats in capsules.[56] Both ligands are approximately 24 times as effective as the parent **2**, with ICE values of 26.7 ± 4.7% (p < 0.001) and 25.9 ± 6.5% (p < 0.001), respectively. The difference in iron clearing properties between **4** and **5** vs **6** and **7** is likely due to the differences in lipophilicity as reflected in the log P_{app} (Table 1). This observation has remained remarkably consistent throughout our studies with DFT analogues.[34,43,45] The latter two ligands are more lipophilic, with larger log P_{app} values.

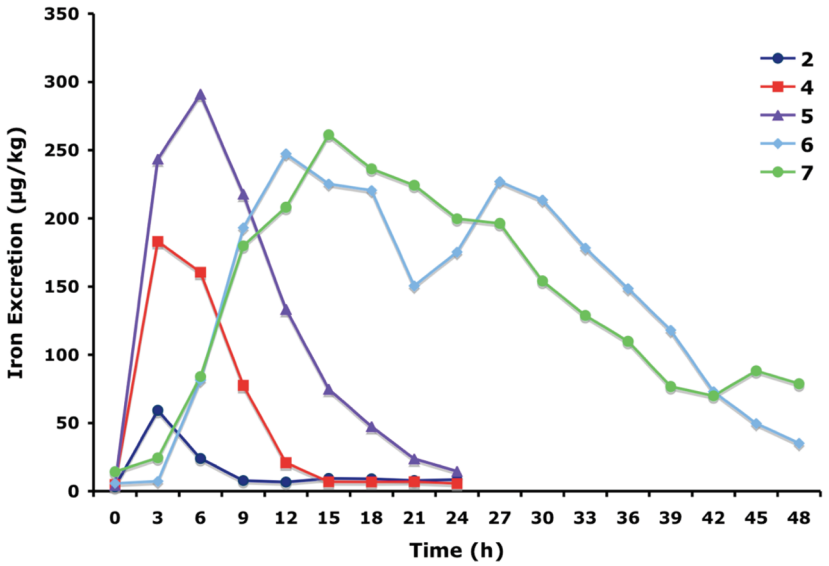

Figure 3. Biliary ferrokinetics of DFT-related chelators **2** and **4**−**7** given orally to non-iron-overloaded, bile duct-cannulated rats at a dose of 300 μmol/kg. The iron excretion (y-axis) is reported as μg of iron per kg body weight.

The biliary ferrokinetics profiles of the ligands, **2** and **4**−**7**, are very different (Figure 3) and clearly related to differences in the polyether backbones. The maximum iron clearance (MIC) of the parent drug, deferitrin (**2**), occurs at 3 h, with iron clearance virtually over at 9 h. The trioxa polyether (**4**) also has an MIC at 3 h, with iron excretion extending out to 12 h. The tetraoxa ether analogue **5** has an MIC at 6 h; iron excretion continues for 24 h. The MIC of the dioxa ether analogue **6** and its corresponding ester **7** do not occur until 12−15 h, and iron excretion had not returned to baseline levels even 48 h postdrug. Note that although the biliary ferrokinetics curve of **6** may appear to be biphasic (Figure 3), the reason for this unusual line shape is that several animals had temporarily obstructed bile flow. While the concentration of iron in the bile remained the same, the bile volume, and thus overall iron excretion, decreased. Once the obstruction was resolved, bile volume and overall iron excretion normalized.

Chelator-Induced Iron Clearance in Iron-Overloaded Primates. The iron clearance data for the chelators in the primates are described in Table 1. We have included historical data (compounds **1**−**4**) for comparative purposes.[34,39,40,42,43] Ligand **2** had an ICE of 16.8 ± 7.2%,[34] while the ICE of **4** is 25.4 ± 7.4%.[34] The ICE of the longer 3,6,9,12-tetraoxa analogue (**5**) was significantly less, 9.8 ± 1.9% ($p < 0.001$). The shorter 3,6-dioxa analogue, **6**, had an ICE of 26.3 ± 9.9% when it was given to the primates in capsules; the ICE was virtually identical when it was administered by gavage as its sodium salt, 28.7 ± 12.4% ($p > 0.05$). The similarity in ICE of **6** between the encapsulated acid and the sodium salt given by gavage suggest comparable pharmacokinetics. The ester of ligand **6**, compound **7**, performed relatively poorly in the primates, with an ICE of only 8.8 ± 2.2%.

There are some very notable differences between the current ICE data and previously reported studies.[34,43,46] In the past, ligands generally performed significantly better in the iron-overloaded primates than in the non-iron-overloaded rodents. For example, we reported that the performance ratio (PR), defined as the mean $ICE_{primates}/ICE_{rodents}$, of analogues **2**−**4** are 15.3, 3.7, and 4.6, respectively (Table 1).[46] In the current study, the PR of ligand **5** is 0.8, while that of **6** is 1.0. Previously, the only ligand that behaved so alike in primates and rodents was the 5′-isomer of **4**, which also had a performance ratio of 1.[46] However, on an absolute basis, the ICE for this chelator in primates (8.1 ± 2.8%) was, in fact, poor. In current study, ligand **6** performed exceptionally well in both rodents and primates (ICE > 26%), suggesting a higher index of success in humans. The ester of **6**, ligand **7**, on the other hand, had a very low performance ratio (0.3), lower than we have previously observed.

The profound difference between the ICE of the parent acid chelator **6** vs that of the ester **7** in rodents and primates is consistent with two possible explanations: (1) the ester is poorly absorbed from the gastrointestinal (GI) tract in the primates, or (2) the primate nonspecific serum esterases simply may not cleave ester **7** to the active chelator acid **6**. An experiment was performed using rat and monkey plasma in an attempt to determine if the relatively poor ICE of **7** in the primates was due to interspecies differences in hydrolysis. When **7** was solubilized in DMSO and incubated at 37 °C with rat plasma, all of the ester had been converted to the active acid **6** within 1−2 h. This was also the case when the experiment was carried out with plasma from the *Cebus apella* monkeys. Thus, there is no difference in the hydrolysis of **7** between the rats and the primates. Therefore, the poor ICE of **7** in the monkeys is consistent with the idea that the ester is absorbed much more effectively from the GI tract of the rodents than from the GI tract of the primates. Control experiments were also performed in which *saline* was used in place of the rat or monkey plasma. Note that when **7** was solubilized in DMSO and incubated with saline in place of the rat or monkey plasma, all of the drug remained in the form of the ester.

Toxicity Profile of (*S*)-4,5-Dihydro-2-[2-hydroxy-4-(3,6-dioxaheptyloxy)phenyl]-4-methyl-4-thiazolecarboxylic Acid (6) and its Ethyl Ester (7). Ten-day toxicity trials have been carried out in rats on both ligands **6** and **7**. The drugs were given to the animals orally once daily at a dose of 384 μmol/kg/d (equivalent to 100 mg/kg/d of DFT sodium salt). Additional

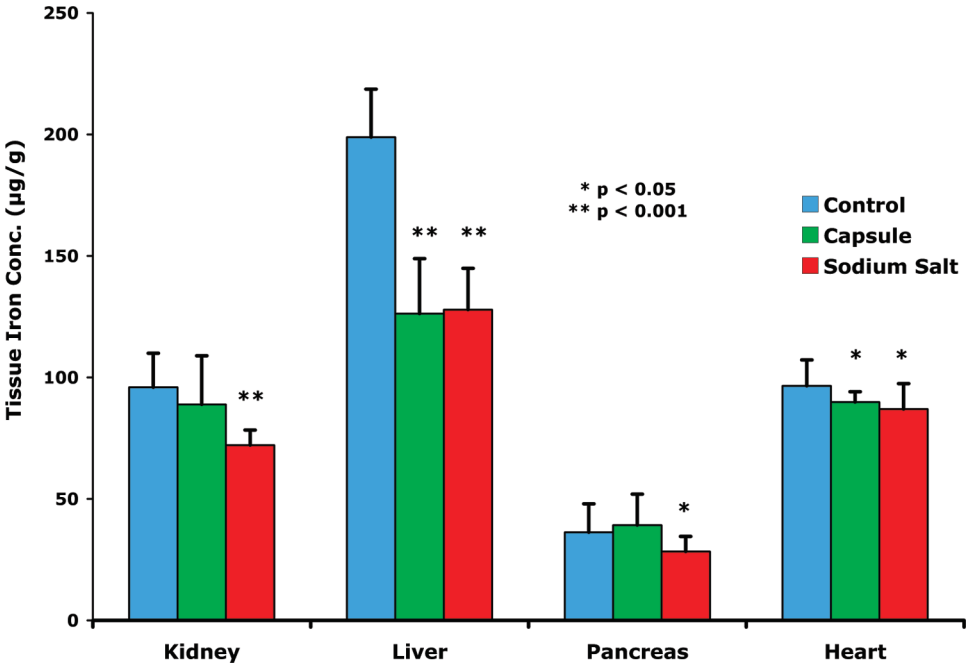

Figure 4. Tissue iron concentration of rats treated with **6** once daily at a dose of 384 μmol/kg/d × 10 d. The chelator was administered orally in gelatin capsules (n = 5) or by gavage as its monosodium salt (n = 10). Age-matched rats (n = 12) served as untreated controls.

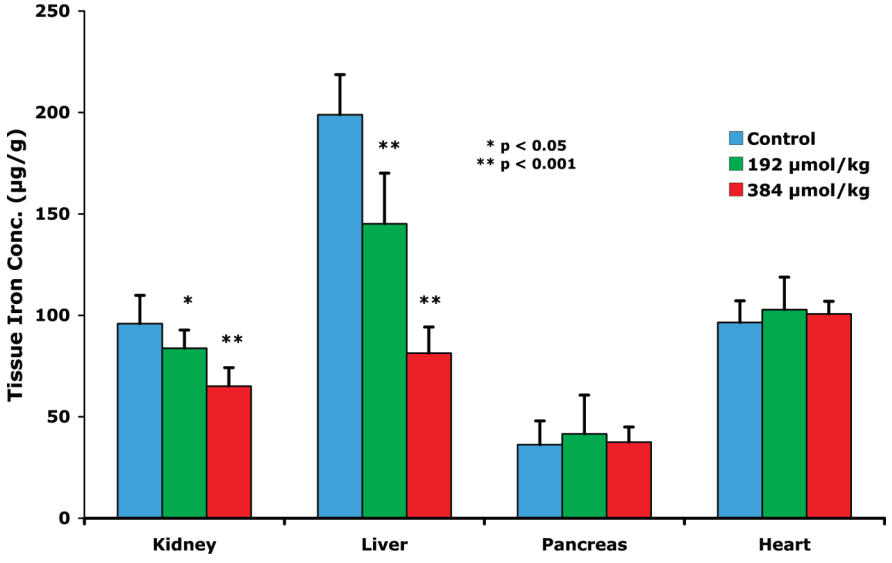

Figure 5. Tissue iron concentration of rats treated with **7** once daily at a dose of 192 (n = 6) or 384 μmol/kg/d (n = 5) × 10 d. The chelator was administered orally in gelatin capsules. Age-matched rats (n = 12) served as untreated controls.

age-matched animals served as untreated controls. The animals were euthanized on day 11, one day after the last dose of drug. Extensive tissues were sent out for histopathological examination. The kidney, liver, pancreas, and heart of test and control animals were removed and wet-ashed to assess their iron content.

Because ligand **6** was such an effective iron chelator in both the rats and the primates, its toxicity profile is most relevant. The key comment from the pathologist was that "The tissues from rats in group 1 [test group] cannot be reliably differentiated histologically from the tissues from rats in group 2 [control animals]." This was very encouraging, especially in view of how much iron the chelator removed from the liver and heart in such a short period of time (discussed below). However, in spite of this outcome, it is clear that any protracted toxicity trials in rodents will have to include groups of both iron-loaded and non-iron-loaded animals, as a 28-day exposure to **6** could reduce the liver iron stores sufficiently to lead to toxicity.

The scenario with the ethyl ester of **6**, compound **7**, was somewhat different. While its ICE was excellent in rodents, along with an impressive reduction in liver and renal iron content (discussed below), ester **7** did present with some renal toxicity. Mild to moderate vacuolar degeneration of the proximal tubular epithelial cells was found when **7** was given at a dose of 384 μmol/kg/d × 10 d. However, when the dose of **7** was reduced to 192 μmol/kg/d × 10 d, there were no drug-related abnormalities.

Tissue Iron Decorporation. As described above, rodents were given acid **6** or **7** orally at a dose of 384 μmol/kg/d × 10 d.

Ethyl ester **7** was also given at a dose of 192 μmol/kg/d × 10 d. On day 11, the animals were euthanized and the kidney, liver, pancreas, and heart were removed. The tissue samples were wet-ashed, and their iron levels were determined, Figures 4 and 5. The renal iron content of rodents treated with **6** was reduced by 7.4% when the drug was administered in capsules and by 24.8% when it given as its sodium salt (Figure 4). Although the renal iron content of the latter animals was significantly less than that of the untreated controls ($p < 0.001$), there was not a significant difference between the capsule or sodium salt groups ($p > 0.05$). The reduction in liver iron was profound, >35% in both the capsule and sodium salt groups ($p < 0.001$). There was a significant reduction in pancreatic iron when the drug was given as its sodium salt ($p < 0.05$) vs the untreated controls, but not when it was dosed in capsules (Figure 4). However, as with the renal iron, there was no significant difference between the capsule vs sodium salt treatment groups ($p > 0.05$). Finally, there was a significant decrease in the cardiac iron of animals treated with acid **6**, 6.9% and 9.9% when the drug was given in capsules and as its sodium salt, respectively ($p < 0.05$).

Rats given the ethyl ester **7** in capsules orally at a dose of 384 μmol/kg/d × 10 d had a profound reduction in both renal and hepatic iron vs the untreated controls, 32.1% ($p < 0.001$) and 59.1% ($p < 0.001$), respectively (Figure 5). We have never observed such a dramatic decrease in tissue iron concentration. Because of the renal toxicity observed with **7** at the 384 μmol/kg/d dosing regimen, we decided to repeat the 10-day toxicity study, this time administering the drug at half of the dose, 192 μmol/kg/d. A clear dose response was observed in the reduction in renal and liver iron concentrations (Figure 5). The kidney iron reduction was 32.1% at 384 μmol/kg/d, and 12.6% at 192 μmol/kg/d ($p < 0.01$). The liver iron reduction was 59.1% at 384 μmol/kg/d and 27% at 192 μmol/kg/d ($p < 0.001$). Neither dose was associated with a reduction in pancreatic or cardiac iron content.

Conclusion

Earlier studies with **2** revealed that methylation of the 4′-hydroxyl resulted in a ligand (**3**) with better ICE in both the rodents and the primates (Table 1).[43] However, ligand **3** was unacceptably nephrotoxic[34] and was reengineered, adding a 3,6,9-trioxadecyl group to the 4′-(HO) in place of the methyl.[34,46,47] This resulted in a chelator (**4**) with about the same ICE in rodents and primates as methylated analogue **3**, but virtually absent of any nephrotoxicity.[34] The corresponding 3′- and the 5′-trioxa analogues also had better ICE properties in rodents than the 4′-*O*-methyl ether **3**. In the primates, the ICE of the 3′-trioxa ligand was similar to that of the 4′-trioxa analogue (**4**), while the 5′- was less effective. These data encouraged an assessment of how altering the *length* of the polyether chain would affect a ligand's ICE, lipophilicity, and physiochemical properties.

The 3,6,9-trioxadecyloxy substituent at the 4′-position of ligand **4**[34] was both lengthened to a 3,6,9,12-tetraoxatridecyloxy group, providing **5**, and shortened to a 3,6-dioxaheptyloxy moiety, providing **6**. In addition, the ethyl (**7**) and isopropyl (**13**) esters of ligand **6** were also generated. The synthetic methodologies were very simple with high yields, an advantage when large quantities of drug are required for preclinical studies.

In all cases, the ethyl ester of **2**, compound **10**, served as the starting material (Schemes 1 and 2). The 4′-(HO) of **10** was alkylated with either polyether iodide **9** or tosylate **12** to afford **11** or **7**, respectively. This was followed by hydrolysis of each ethyl ester in aqueous base, providing **5** (an oil) with a longer polyether chain (Scheme 1), or ligand **6**, possessing a shorter polyether chain (Scheme 2). Both **6** and its ester **7** are crystalline solids. The toxicity profile, efficacy as an iron-clearing agent, and physiochemical state, a crystalline solid, make ligand **6** a very attractive clinical candidate. The fact that the ethyl ester of **6**, masked ligand **7**, also readily crystallizes is remarkable (see X-ray structures, Figures 1 and 2). All polyether analogues previously synthesized by this laboratory, both acids and esters, were oils.[34,46,47] In most instances, metal salts of the former were hygroscopic. Interestingly, even the isopropyl ester of **6**, compound **13**, was an oil. Because **6** and **7** are crystalline solids, they were given in capsules[56] to both the rodents and the primates.

In rodents, the ICE of **5** as its sodium salt was nearly 11 times greater than that of the parent (**2**) and twice as effective as the trioxa polyether (**4**). The shorter polyether acid **6** given in capsules had an ICE that was 24 times greater than **2** and was nearly five times greater than that of **4** (Table 1). The ICE of the corresponding ester **7** was virtually identical to that of **6**. The biliary ferrokinetics curves for both **6** and **7** were profoundly different than any of the other ligands (Figure 3). MIC did not occur until 12−15 h postdrug, and iron clearance was still ongoing even at 48 h. In contrast, MIC occurred much earlier with the other ligands, 3 h for **2** and **4**, and 6 h for **5**. In addition, iron excretion had returned to baseline levels by 9 h for **2**, 12 h for **4**, and 24 h for **5** (Figure 3). If the protracted iron clearance properties of ligand **6** were also observed in humans, thalassemia patients may only need to be treated two to three times a week. This would be an improvement over the rigors of the currently available treatment regimens.

In primates, the ICE of the parent polyether **4** was 2.5 greater than that of the longer analogue **5**, while the ICE of the shorter polyether analogue **6** was within error of that of **4** (Table 1). However, the ICE of the ethyl ester of **6**, ligand **7**, is only one-third that of **6** (Table 1). Studies in rat and monkey plasma suggested no difference in the nonspecific esterase hydrolysis of **7** between the rats and the primates. The poor ICE of **7** in the monkeys is, however, consistent with the idea that the ester is absorbed much more effectively from the GI tract in rodents than in primates.

The protracted biliary ferrokinetics and outstanding iron clearing efficiencies of polyether acid **6** and ester **7** noted in the bile duct-cannulated rats (Figure 3) were reflected in a dramatic reduction in the tissue iron levels of rodents treated orally with the drugs once daily for 10 days (Figures 4 and 5). Acid **6**, given orally in capsules or by gavage as its sodium salt, significantly reduced both hepatic and cardiac iron (Figure 4) with no histological abnormalities noted between the treated and the control groups. Compound **7** administered in capsules decorporated even more iron from the kidney and liver than **6** but had no impact on pancreatic or cardiac iron burden (Figure 5). However, this is probably a moot point, as ester **7** presented with unacceptable renal toxicity.

Compound **11** (Scheme 1), the ethyl ester of chelator **5** (Table 1), was an intermediate in the synthesis of **5**. We elected not to evaluate ester **11** because the parent acid itself did not perform well in primates. The ester, even if cleaved to the acid **5** in animals by nonspecific serum esterases, would not be expected to perform any better than the parent acid itself. This is underscored when comparing acid **6** (Table 1) with its

ester **7** (Table 1). This ester does not work as well in primates as the parent acid. This is also why we elected not to evaluate ester **13**. The synthesis of **13** was simply to assess whether esters other than the ethyl ester of **7** could also be expected to be solids.

The outcome of the study clearly demonstrates that altering the length of the 4′-polyether backbone can have a profound effect on the ligand's ICE, biliary ferrokinetics, and physiochemical properties. The results strongly suggest that the 3,6-dioxaheptyloxy polyether ligand (**6**) should be pursued further as a clinical candidate.

Experimental Section

Materials. Reagents were purchased from Aldrich Chemical Co. (Milwaukee, WI). Fisher Optima grade solvents were routinely used, and DMF was distilled. Reactions were run under a nitrogen atmosphere, and organic extracts were dried with sodium sulfate. Silica gel 40−63 from SiliCycle, Inc. (Quebec City, Quebec, Canada) was used for column chromatography. Melting points are uncorrected. Glassware that was presoaked in 3 N HCl for 15 min, washed with distilled water and distilled EtOH, and oven-dried was used during the isolation of **5** and **6**. Optical rotations were run at 589 nm (sodium D line) and 20 °C on a Perkin-Elmer 341 polarimeter, with *c* being concentration in grams of compound per 100 mL of $CHCl_3$. ^{1}H NMR spectra were run in $CDCl_3$ at 400 MHz, and chemical shifts (δ) are given in parts per million downfield from tetramethylsilane. Coupling constants (*J*) are in hertz. ^{13}C NMR spectra were measured in $CDCl_3$ at 100 MHz, and chemical shifts (δ) are given in parts per million referenced to the residual solvent resonance of δ 77.16. The base peaks are reported for the ESI-FTICR mass spectra. Elemental analyses were performed by Atlantic Microlabs (Norcross, GA) and were within ±0.4% of the calculated values. Purity of the compounds is supported by elemental analyses and high pressure liquid chromatography (HPLC). In every instance, the purity was ≥95%.

Cebus apella monkeys were obtained from World Wide Primates (Miami, FL). Male Sprague−Dawley rats were procured from Harlan Sprague−Dawley (Indianapolis, IN). Ultrapure salts were obtained from Johnson Matthey Electronics (Royston, UK). All hematological and biochemical studies[41] were performed by Antech Diagnostics (Tampa, FL). Atomic absorption (AA) measurements were made on a Perkin-Elmer model 5100 PC (Norwalk, CT). Histopathological analysis was carried out by Florida Vet Path (Bushnell, FL).

X-ray Experimental. Data for **6** and **7** were collected at 173 K on a Siemens SMART PLATFORM equipped with a CCD area detector and a graphite monochromator utilizing MoK_α radiation (λ = 0.71073 Å). Cell parameters were refined using up to 8192 reflections. A full sphere of data (1850 frames) was collected using the ω-scan method (0.3° frame width). The first 50 frames were remeasured at the end of data collection to monitor instrument and crystal capability (maximum correction on *I* was <1%). Absorption corrections by integration were applied based on measured indexed crystal faces.

The structures were solved by the Direct Methods in SHELXTL6[57] and refined using full-matrix least-squares. The non-H atoms were treated anisotropically, whereas the hydrogen atoms were calculated in ideal positions and were riding on their respective carbon atoms. For **6**, a total of 227 parameters were refined in the final cycle of refinement using 3588 reflections with $I > 2\sigma(I)$ to yield R_1 and wR_2 of 3.16% and 8.58%, respectively. For compound **7**, a total of 243 parameters were refined in the final cycle of refinement using 4082 reflections with $I > 2\sigma(I)$ to yield R_1 and wR_2 of 2.52% and 6.53%, respectively. Refinements were done using F^2. Full crystallographic data for **6** and **7** have been submitted to CCDC (deposition nos. CCDC 757291 and 757292).

Synthetic Methods. (*S*)-4,5-Dihydro-2-[2-hydroxy-4-(3,6,9,12-tetraoxatridecyloxy)phenyl]-4-methyl-4-thiazolecarboxylic Acid (5). A solution of 50% (w/w) NaOH (7.0 g, 87 mmol) in CH_3OH (75 mL) was added to **11** (3.64 g, 7.72 mmol) in CH_3OH (85 mL) at 0 °C over 3 min. The reaction mixture was stirred at 0 °C for 1.5 h and at room temperature for 18 h, and the bulk of the solvent was removed under reduced pressure. The residue was treated with H_2O (90 mL) and was extracted with $CHCl_3$ (4 × 50 mL). The aqueous layer was cooled in ice, combined with saturated NaCl (45 mL) and cold 5 N HCl (22 mL), and was extracted with EtOAc (100 mL, 5 × 70 mL). The EtOAc layers were washed with saturated NaCl (75 mL). Solvent was removed in vacuo, affording 3.20 g of **5** (94%) as a yellow oil: [α] +47.6° (*c* 0.86). ^{1}H NMR ($CDCl_3$ + 1−2 drops D_2O) δ 1.69 (s, 3 H), 3.21 (d, 1 H, *J* = 11.3), 3.38 (s, 3 H), 3.53−3.57 (m, 2 H), 3.62−3.69 (m, 8 H), 3.70−3.73 (m, 2 H), 3.82−3.87 (m, 3 H), 4.11−4.15 (m, 2 H), 6.45 (dd, 1 H, *J* = 8.8, 2.5), 6.50 (d, 1 H, *J* = 2.4), 7.27 (d, 1 H, *J* = 9.0). ^{13}C NMR δ 24.67, 39.90, 59.11, 69.66, 70.53, 70.67, 70.69, 70.71, 70.94, 72.02, 82.93, 101.56, 107.70, 109.80, 131.85, 161.32, 163.30, 171.76, 176.19. HRMS *m*/*z* calcd for $C_{20}H_{30}NO_8S$, 444.1687 (M + H); found, 444.1691. Anal. ($C_{20}H_{29}NO_8S$) C, H, N.

(*S*)-4,5-Dihydro-2-[2-hydroxy-4-(3,6-dioxaheptyloxy)phenyl]-4-methyl-4-thiazolecarboxylic Acid (6). A solution of 50% (w/w) NaOH (2.1 mL, 40 mmol) in CH_3OH (20 mL) was added to **7** (1.2 g, 3.1 mmol) in CH_3OH (30 mL) at 0 °C. The reaction mixture was stirred at room temperature for 6 h, and the bulk of the solvent was removed under reduced pressure. The residue was treated with dilute NaCl (30 mL) and was extracted with ether (2 × 20 mL). The aqueous layer was cooled in ice, acidified with 6 N HCl to pH = 2, and extracted with EtOAc (4 × 25 mL). The EtOAc layers were washed with saturated NaCl (50 mL). Solvent was removed in vacuo, and recrystallization from EtOAc/hexanes furnished 0.880 g of **6** (80%) as a solid, mp 82−83 °C: [α] +59.6° (*c* 0.094). ^{1}H NMR δ 1.70 (s, 3 H), 3.22 (d, 1 H, *J* = 11.2), 3.40 (s, 3 H), 3.58−3.60 (m, 2 H), 3.71−3.73 (m, 2 H), 3.83−3.87 (m + d, 3 H, *J* = 12.0), 4.15 (t, 2 H, *J* = 5.2), 6.45 (dd, 1 H, *J* = 8.8, 2.0), 6.51 (d, 1 H, *J* = 2.0), 7.28 (d, 1 H, *J* = 8.4). ^{13}C NMR δ 24.58, 39.77, 59.13, 67.64, 69.61, 70.77, 71.99, 82.63, 101.53, 107.73, 109.63, 131.88, 161.42, 163.40, 171.96, 176.91. HRMS *m*/*z* calcd for $C_{16}H_{22}NO_6S$, 356.1162 (M + H); found, 356.1190. Anal. ($C_{16}H_{21}NO_6S$) C, H, N.

Ethyl (*S*)-4,5-Dihydro-2-[2-hydroxy-4-(3,6-dioxaheptyloxy)phenyl]-4-methyl-4-thiazolecarboxylate (7). Flame activated K_2CO_3 (2.16 g, 15.6 mmol) and **12**[49] (3.97 g, 14.5 mmol) were added to **10**[48] (4.0 g, 14.2 mmol) in acetone (100 mL). The reaction mixture was heated at reflux for 2 d. After cooling to room temperature, the solids were filtered and washed with acetone, and the filtrate was concentrated by rotary evaporation. The residue was treated with 1:1 0.5 M citric acid/saturated NaCl (100 mL) and was extracted with EtOAc (3 × 50 mL). The organic extracts were washed with H_2O (100 mL) and saturated NaCl (100 mL). After solvent was removed in vacuo, recrystallization from EtOAc/hexanes furnished 3.97 g of **7** (73%) as a solid, mp 68−70 °C: [α] +47.4° (*c* 0.114). ^{1}H NMR δ 1.30 (t, 3 H, *J* = 7.2), 1.66 (s, 3 H), 3.19 (d, 1 H, *J* = 11.2), 3.40 (s, 3 H), 3.57−3.59 (m, 2 H), 3.71−3.73 (m, 2 H), 3.83−3.88 (d + m, 3 H, *J* = 11.6), 4.16 (t, 2 H, *J* = 4.8), 4.24 (dq, 2 H, *J* = 7.2, 1.6), 6.46 (dd, 1 H, *J* = 8.8, 2.4), 6.49 (d, 1 H, *J* = 2.8), 7.29 (d, 1 H, *J* = 8.4), 12.69 (s, 1 H). ^{13}C NMR δ 14.12, 24.48, 39.84, 59.09, 61.89, 67.55, 69.52, 70.80, 71.94, 83.12, 101.45, 107.28, 109.89, 131.69, 161.18, 162.99, 170.81, 172.80. HRMS *m*/*z* calcd for $C_{18}H_{26}NO_6S$, 384.1475 (M + H); found, 384.1509. Anal. ($C_{18}H_{25}NO_6S$) C, H, N.

13-Iodo-2,5,8,11-tetraoxatridecane (9). Sodium iodide (8.61 g, 57.5 mmol) was added to a solution of **8** (10.37 g, 28.61 mmol) in acetone (230 mL), and the reaction mixture was heated at reflux for 18 h. After the solvent was evaporated in vacuo, the residue was combined with H_2O (150 mL) and was extracted with CH_2Cl_2 (150 mL, 2 × 80 mL). The organic extracts were washed with 1% $NaHSO_3$ (80 mL), H_2O (80 mL), and saturated NaCl

(50 mL), and solvent was evaporated in vacuo. Purification by flash column chromatography using 14% acetone/CH_2Cl_2 generated 8.56 g of **9** (94%) as a colorless liquid: ^{1}H NMR δ 3.24−3.29 (m, 2 H), 3.39 (s, 3 H), 3.54−3.58 (m, 2 H), 3.64−3.70 (m, 10 H), 3.74−3.78 (m, 2 H). ^{13}C NMR δ 59.17, 70.32, 70.65, 70.70, 70.73, 70.77, 72.05, 72.09. HRMS *m*/*z* calcd for $C_9H_{20}IO_4$, 319.0401 (M + H); found, 319.0417. Anal. ($C_9H_{19}IO_4$) C, H.

Ethyl (*S*)-4,5-Dihydro-2-[2-hydroxy-4-(3,6,9,12-tetraoxatridecyloxy)phenyl]-4-methyl-4-thiazolecarboxylate (11). Flame activated K_2CO_3 (0.666 g, 4.82 mmol) was added to a solution of **9** (1.46 g, 4.59 mmol) and **10**[48] (1.08 g, 3.84 mmol) in acetone (85 mL), and the reaction mixture was heated at reflux for 43 h. After cooling to room temperature, the solids were filtered and washed with acetone, and the filtrate was concentrated by rotary evaporation. The residue was combined with 1:1 0.5 M citric acid/saturated NaCl (100 mL) and was extracted with EtOAc (3 × 80 mL). The organic extracts were washed with 1% $NaHSO_3$ (80 mL), H_2O (80 mL) and saturated NaCl (55 mL). After solvent was removed in vacuo, the residue was purified by flash column chromatography eluting with 25% acetone/petroleum ether then 9% acetone/CH_2Cl_2, furnishing 1.33 g of **11** (73%) as a yellow oil: [α] +36.2° (*c* 1.20). ^{1}H NMR δ 1.30 (t, 3 H, *J* = 7.2), 1.66 (s, 3 H), 3.19 (d, 1 H, *J* = 11.3), 3.38 (s, 3 H), 3.52−3.56 (m, 2 H), 3.62−3.74 (m, 10 H), 3.81−3.88 (m, 3 H), 4.12−4.16 (m, 2 H), 4.20−4.28 (m, 2 H), 6.46 (dd, 1 H, *J* = 8.6, 2.3), 6.49 (d, 1 H, *J* = 2.4), 7.29 (d, 1 H, *J* = 8.6). ^{13}C NMR δ 14.21, 24.59, 39.95, 59.14, 62.01, 67.66, 69.58, 70.62, 70.71, 70.73, 70.97, 72.04, 83.23, 101.52, 107.42, 109.99, 131.78, 161.28, 163.11, 170.90, 172.95. HRMS *m*/*z* calcd for $C_{22}H_{34}NO_8S$, 472.2000 (M + H); found, 472.2007. Anal. ($C_{22}H_{33}NO_8S$) C, H, N.

Isopropyl (*S*)-4,5-Dihydro-2-[2-hydroxy-4-(3,6-dioxaheptyloxy)-phenyl]-4-methyl-4-thiazolecarboxylate (13). 2-Iodopropane (1.60 g, 9.41 mmol) and DIEA (1.22 g, 9.44 mmol) were successively added to **6** (2.1 g, 5.9 mmol) in DMF (50 mL), and the reaction mixture was stirred at room temperature for 72 h. After solvent removal under high vacuum, the residue was treated with 1:1 0.5 M citric acid/saturated NaCl (100 mL) and was extracted with EtOAc (3 × 100 mL). The organic extracts were washed with 50 mL portions of 1% $NaHSO_3$, H_2O, and saturated NaCl, and solvent was evaporated in vacuo. Purification by flash column chromatography using 5% acetone/CH_2Cl_2 generated 1.99 g of **13** (85%) as a yellow oil: [α] +40.0° (*c* 0.125). ^{1}H NMR δ 1.26 and 1.27 (2 d, 6 H, *J* = 5.5), 1.63 (s, 3 H), 3.17 (d, 1 H, *J* = 11.2), 3.38 (s, 3 H), 3.55−3.58 (m, 2 H), 3.69−3.72 (m, 2 H), 3.81−3.86 (d + m, 3 H, *J* = 11.2), 4.15 (t, 2 H, *J* = 5.2), 5.07 (septet, 1 H, *J* = 6.4), 6.46 (dd, 1 H, *J* = 9.2, 2.0), 6.49 (d, 1 H, *J* = 2.4), 7.28 (d, 1 H, *J* = 8.4), 12.7 (br s, 1 H). ^{13}C NMR δ 21.54, 24.27, 39.63, 58.98, 67.46, 69.35, 69.42, 70.69, 71.85, 83.10, 101.37, 107.14, 109.83, 131.57, 161.11, 162.88, 170.55, 172.10. HRMS *m*/*z* calcd for $C_{19}H_{28}NO_6S$, 398.1637 (M + H); found, 398.1658. Anal. ($C_{19}H_{27}NO_6S$) C, H, N.

Biological Methods. Cannulation of Bile Duct in Non Iron-Overloaded Rats. The cannulation has been described previously.[40,41,58] Bile samples were collected from male Sprague−Dawley rats (400−450 g) at 3 h intervals for up to 48 h. The urine sample(s) was taken at 24 h intervals. Sample collection and handling are as previously described.[40,41]

Iron Loading of *C. apella* Monkeys. The monkeys (3.5−4 kg) were iron overloaded with intravenous iron dextran as specified in earlier publications to provide about 500 mg of iron per kg of body weight;[40,59] the serum transferrin iron saturation rose to between 70 and 80%. At least 20 half-lives, 60 days,[60] elapsed before any of the animals were used in experiments evaluating iron-chelating agents.

Primate Fecal and Urine Samples. Fecal and urine samples were collected at 24 h intervals and processed as described previously.[40,41,61] Briefly, the collections began 4 days prior to the administration of the test drug and continued for an additional 5 days after the drug was given. Iron concentrations were determined by flame absorption spectroscopy as presented in other publications.[40,62]

Drug Preparation and Administration. In the iron clearing experiments, the rats were given **5**−**7** orally at a dose of 300 μmol/kg. Ligand **5** was given by gavage as its monosodium salt (prepared by the addition of 1 equiv of NaOH to a suspension of the free acid in distilled water), while **6** and **7** were given in capsules. The primates were given **5**−**7** orally at a dose of 75 μmol/kg. Ligand **5** was given to the primates by gavage as its monosodium salt. Analogue **6** was given to the monkeys by gavage as its monosodium salt, as well as in capsules. Ligand **7** was given to the monkeys in capsules. Drug preparation for the rodent toxicity studies of **6** and **7** are described below.

Calculation of Iron Chelator Efficiency. The theoretical iron outputs of the chelators were generated on the basis of a 2:1 ligand:iron complex. The efficiencies in the rats and monkeys were calculated as set forth elsewhere.[42,58] Data are presented as the mean ± the standard error of the mean; *p*-values were generated via a one-tailed Student's *t*-test in which the inequality of variances was assumed, and a *p*-value of <0.05 was considered significant.

Plasma Analytical Methods. Analytical separation was performed on a Discovery RP Amide C16 HPLC system with a Shimadzu SPD-10A UV−vis detector at 310 nm as previously described.[51,58] Mobile phase and chromatographic conditions were as follows. Mobile phase A (MPA): 25 mM KH_2PO_4 + 2.5 mM 1-octanesulfonic acid, pH 3 (95%) and acetonitrile (5%); mobile phase B (MPB): 25 mM KH_2PO_4 + 2.5 mM 1-octanesulfonic acid, pH 3 (40%) and acetonitrile (60%). The chelator concentrations were calculated from the peak area fitted to calibration curves by nonweighted least-squares linear regression with Shimadzu CLASS-NP 7.4 chromatography software. The method had a detection limit of 0.1 μM and was reproducible and linear over a range of 0.2−20 μM.

The ethyl ester (**7**) was solubilized in DMSO and further diluted with distilled water to provide a 100 μM solution. A 25 μL aliquot of the drug solution was added to centrifuge tubes containing 100 μL of rat or primate plasma. Control experiments were also performed in which *saline* was used in place of the rat or monkey plasma. The centrifuge tubes were vortexed and incubated in a shaking incubator at 37 °C for 1 or 2 h. Note that separate samples were processed for each species at each time point (four samples total). Methanol (400 μL) was added to the centrifuge tubes at the end of the incubation period to stop the reaction. The tubes were stored at −20 °C for at least 0.5 h. The tubes were then allowed to warm to room temperature. The samples were vortexed and centrifuged for 10 min at 10000 rpm. Supernatant (100 μL) was diluted with MPA (minus the 1-octanesulfonic acid, 400 μL), vortexed, and run on the HPLC as usual.

Toxicity Evaluation of 6 and 7 in Rodents. Male Sprague−Dawley rats (300−350 g) were fasted overnight and were given the chelators first thing in the morning. The rats were fed ∼3 h postdrug and had access to food for ∼5 h before being fasted overnight. Ligand **6** was given to the rats orally once daily at a dose of 384 μmol/kg/d × 10 d. Note that this dose is equivalent to 100 mg/kg/d of the DFT sodium salt. The chelator (**6**) was administered orally in gelatin capsules (n = 5), or by gavage as its monosodium salt (n = 10). The ethyl ester (**7**) was administered orally in capsules once daily at a dose of 192 (n = 6) or 384 μmol/kg/d (n = 5) × 10 d. Age-matched rats (n = 12) served as untreated controls. The rats were euthanized 24 h postdrug (day 11) and extensive tissues were collected for histopathological analysis. Samples of the kidney, liver, heart, and pancreas were reserved and assessed for their iron content.

Preparation of Rodent Tissues for the Determination of their Iron Content. The initial step in the tissue preparation involved removing any obvious membranes or fat. A sample of each

tissue (300−350 mg) was weighed and transferred to acid-washed hydrolysis (pressure) tubes. Note that the same region of each tissue was always utilized. Concentrated HNO_3 (65%), 1.5 mL, and distilled water (2 mL) were added. The tubes were then sealed and placed in a 120 °C oil bath for 5 h; the tubes were vented as necessary. Then, the tubes were removed from the oil bath and allowed to cool to room temperature. The temperature of the oil bath was decreased to 100 °C. Once the samples were cooled, 0.7 mL of hydrogen peroxide (30%) was added to the hydrolysis tube. The samples were placed back in the oil bath and cooked overnight. The samples were then removed from the oil bath and allowed to cool to room temperature. The hydrolysis tubes were vortexed, and the digested samples were poured into 50 mL volumetric flasks. The samples were brought to volume using distilled water. Finally, the samples were poured into a syringe and filtered using 0.45 μ, 30 mm, Teflon syringe filters. Iron concentrations were determined by flame absorption spectroscopy as presented in other publications.[40,41]

Acknowledgment. The project described was supported by grant number R37DK049108 from the National Institute of Diabetes and Digestive and Kidney Diseases. The content is solely the responsibility of the authors and does not necessarily represent the official views of the National Institute of Diabetes and Digestive and Kidney Diseases or the National Institutes of Health. We thank Elizabeth M. Nelson and Katie Ratliff-Thompson for their technical assistance and Miranda E. Coger for her editorial and organizational support. K.A.A. acknowledges the National Science Foundation and the University of Florida for funding of the purchase of the X-ray equipment. We acknowledge the spectroscopy services in the Chemistry Department, University of Florida, for the mass spectrometry analyses.

Supporting Information Available: Elemental analytical data for synthesized compounds, X-ray crystallographic data collection and refinement parameters along with selected bond angles and lengths for compounds **6** and **7**. This material is available free of charge via the Internet at http://pubs.acs.org.

References

(1) Graf, E; Mahoney, J. R.; Bryant, R. G.; Eaton, J. W. Iron-Catalyzed Hydroxyl Radical Formation. Stringent Requirement for Free Iron Coordination Site. *J. Biol. Chem.* **1984**, *259*, 3620–3624.

(2) Halliwell, B. Free Radicals and Antioxidants: A Personal View. *Nutr. Rev.* **1994**, *52*, 253–265.

(3) Halliwell, B. Iron, Oxidative Damage, and Chelating Agents. In *The Development of Iron Chelators for Clinical Use*; Bergeron, R. J., Brittenham, G. M., Eds.; CRC: Boca Raton, FL, 1994; pp 33−56.

(4) Koppenol, W. Kinetics and Mechanism of the Fenton Reaction: Implications for Iron Toxicity. In *Iron Chelators: New Development Strategies*; Badman, D. G., Bergeron, R. J., Brittenham, G. M., Eds.; Saratoga: Ponte Vedra Beach, FL, 2000, pp 3−10.

(5) Babbs, C. F. Oxygen Radicals in Ulcerative Colitis. *Free Radical Biol. Med.* **1992**, *13*, 169–181.

(6) Hazen, S. L.; d'Avignon, A.; Anderson, M. M.; Hsu, F. F.; Heinecke, J. W. Human Neutrophils Employ the Myeloperoxidase-Hydrogen Peroxide−Chloride System to Oxidize α-Amino Acids to a Family of Reactive Aldehydes. Mechanistic Studies Identifying Labile Intermediates along the Reaction Pathway. *J. Biol. Chem.* **1998**, *273*, 4997–5005.

(7) Millán, M; Sobrino, T.; Arenillas, J. F.; Rodríguez-Yáñez, M.; García, M.; Nombela, F.; Castellanos, M.; de la Ossa, N. P.; Cuadras, P.; Serena, J.; Castillo, J.; Dávalos, A. Biological Signatures of Brain Damage Associated with High Serum Ferritin Levels in Patients with Acute Ischemic Stroke and Thrombolytic Treatment. *Dis. Markers* **2008**, *25*, 181–188.

(8) Zecca, L.; Casella, L.; Albertini, A.; Bellei, C.; Zucca, F. A.; Engelen, M.; Zadlo, A.; Szewczyk, G.; Zareba, M.; Sarna, T. Neuromelanin Can Protect Against Iron-Mediated Oxidative Damage in System Modeling Iron Overload of Brain Aging and Parkinson's Disease. *J. Neurochem.* **2008**, *106*, 1866–1875.

(9) Pietrangelo, A. Iron Chelation beyond Transfusion Iron Overload. *Am. J. Hematol.* **2007**, *82*, 1142–1146.

(10) Pippard, M. J. Iron Overload and Iron Chelation Therapy in Thalassaemia and Sickle Cell Haemoglobinopathies. *Acta. Haematol.* **1987**, *78*, 206–211.

(11) Olivieri, N. F. Progression of Iron Overload in Sickle Cell Disease. *Semin. Hematol.* **2001**, *38*, 57–62.

(12) Malcovati, L. Impact of Transfusion Dependency and Secondary Iron Overload on the Survival of Patients with Myelodysplastic Syndromes. *Leukemia Res.* **2007**, *31*, S2–S6.

(13) Angelucci, E.; Brittenham, G. M.; McLaren, C. E.; Ripalti, M.; Baronciani, D.; Giardini, C.; Galimberti, M.; Polchi, P.; Lucarelli, G. Hepatic Iron Concentration and Total Body Iron Stores in Thalassemia Major. *N. Engl. J. Med.* **2000**, *343*, 327–331.

(14) Bonkovsky, H. L.; Lambrecht, R. W. Iron-Induced Liver Injury. *Clin. Liver Dis.* **2000**, *4*, 409−429, vi−vii.

(15) Peitrangelo, A. Mechanism of Iron Toxicity. *Adv. Exp. Med. Biol.* **2002**, *509*, 19–43.

(16) Cario, H.; Holl, R. W.; Debatin, K. M.; Kohne, E. Insulin Sensitivity and β-Cell Secretion in Thalassemia Major with Secondary Haemochromatosis: Assessment by Oral Glucose Tolerance Test. *Eur. J. Pediatr.* **2004**, *162*, 139–146.

(17) Wojcik, J. P.; Speechley, M. R.; Kertesz, A. E.; Chakrabarti, S.; Adams, P. C. Natural History of C282Y Homozygotes for Haemochromatosis. *Can. J. Gastroenterol.* **2002**, *16*, 297–302.

(18) Brittenham, G. M. Disorders of Iron Metabolism: Iron Deficiency and Overload. In *Hematology: Basic Principles and Practice*, 3rd ed.; Hoffman, R., Benz, E. J., Shattil, S. J. Furie, B., Cohen, H. J., et al., Eds.; Churchill Livingstone: New York, 2000; pp 397−428.

(19) Brittenham, G. M.; Griffith, P. M.; Nienhuis, A. W.; McLaren, C. E.; Young, N. S.; Tucker, E. E.; Allen, C. J.; Farrell, D. E.; Harris, J. W. Efficacy of Deferoxamine in Preventing Complications of Iron Overload in Patients with Thalassemia Major. *N. Engl. J. Med.* **1994**, *331*, 567–573.

(20) Zurlo, M. G.; De Stefano, P.; Borgna-Pignatti, C.; Di Palma, A.; Piga, A.; Melevendi, C.; Di Gregorio, F.; Burattini, M. G.; Terzoli, S. Survival and Causes of Death in Thalassemia Major. *Lancet* **1989**, *2*, 27–30.

(21) *Desferal*; Novartis Pharmaceuticals Corporation: East Hanover, NJ, **2008**; http://www.pharma.us.novartis.com/product/pi/pdf/desferal.pdf.

(22) Hoffbrand, A. V.; Al-Refaie, F.; Davis, B.; Siritanakatkul, N.; Jackson, B. F. A.; Cochrane, J.; Prescott, E.; Wonke, B. Long-Term Trial of Deferiprone in 51 Transfusion-Dependent Iron Overloaded Patients. *Blood* **1998**, *91*, 295–300.

(23) Olivieri, N. F. Long-Term Therapy with Deferiprone. *Acta Haematol.* **1996**, *95*, 37–48.

(24) Olivieri, N. F.; Brittenham, G. M.; McLaren, C. E.; Templeton, D. M.; Cameron, R. G.; McClelland, R. A.; Burt, A. D.; Fleming, K. A. Long-Term Safety and Effectiveness of Iron-Chelation Therapy with Deferiprone for Thalassemia Major. *N. Engl. J. Med.* **1998**, *339*, 417–423.

(25) Richardson, D. R. The Controversial Role of Deferiprone in the Treatment of Thalassemia. *J. Lab. Clin. Med.* **2001**, *137*, 324–329.

(26) Nisbet-Brown, E.; Olivieri, N. F.; Giardina, P. J.; Grady, R. W.; Neufeld, E. J.; Sechaud, R.; Krebs-Brown, A. J.; Anderson, J. R.; Alberti, D.; Sizer, K. C.; Nathan, D. G. Effectiveness and Safety of ICL670 in Iron-Loaded Patients with Thalassaemia: A Randomised, Double-Blind, Placebo-Controlled, Dose-Escalation Trial. *Lancet* **2003**, *361*, 1597–1602.

(27) Galanello, R.; Piga, A.; Alberti, D.; Rouan, M.-C.; Bigler, H.; Séchaud, R. Safety, Tolerability, and Pharmacokinetics of ICL670, a New Orally Active Iron-Chelating Agent in Patients with Transfusion-Dependent Iron Overload Due to β-Thalassemia. *J. Clin. Pharmacol.* **2003**, *43*, 565–572.

(28) Cappellini, M. D. Iron-Chelating Therapy with the New Oral Agent ICL670 (Exjade). *Best Pract. Res. Clin. Haematol.* **2005**, *18*, 289–298.

(29) *Exjade Prescribing Information*; Novartis Pharmaceuticals Corporation: East Hanover, NJ, December, **2007**; http://www.pharma.us.novartis.com/product/pi/pdf/exjade.pdf.

(30) Galanello, R.; Forni, G.; Jones, A.; Kelly, A.; Willemsen, A.; He, X.; Johnston, A.; Fuller, D.; Donovan, J.; Piga, A. A Dose Escalation Study of the Pharmacokinetics, Safety and Efficacy of Deferitrin, an Oral Iron Chelator in Beta Thalassaemia Patients. *ASH Annu. Meet. Abstr.* **2007**, *110*, 2669.

(31) Pippard, M. J. Desferrioxamine-Induced Iron Excretion in Humans. *Bailliere's Clin. Haematol.* **1989**, *2*, 323–343.

(32) Giardina, P. J.; Grady, R. W. Chelation Therapy in β-Thalassemia: An Optimistic Update. *Semin. Hematol.* **2001**, *38*, 360–366.

(33) Olivieri, N. F.; Brittenham, G. M. Iron-Chelating Therapy and the Treatment of Thalassemia. *Blood* **1997**, *89*, 739–761.
(34) Bergeron, R. J.; Wiegand, J.; McManis, J. S.; Vinson, J. R. T.; Yao, H.; Bharti, N.; Rocca, J. R. (*S*)-4,5-Dihydro-2-(2-hydroxy-4-hydroxyphenyl)-4-methyl-4-thiazolecarboxylic Acid Polyethers: A Solution to Nephrotoxicity. *J. Med. Chem.* **2006**, *49*, 2772–2783.
(35) Brittenham, G. M. Pyridoxal Isonicotinoyl Hydrazone. Effective Iron Chelation after Oral Administration. *Ann. N. Y. Acad. Sci.* **1990**, *612*, 315–326.
(36) Naegeli, H.-U.; Zähner, H. Metabolites of Microorganisms. Part 193. Ferrithiocin. *Helv. Chim. Acta* **1980**, *63*, 1400–1406.
(37) Hahn, F. E.; McMurry, T. J.; Hugi, A.; Raymond, K. N. Coordination Chemistry of Microbial Iron Transport. 42. Structural and Spectroscopic Characterization of Diastereomeric Cr(III) and Co(III) Complexes of Desferriferrithiocin. *J. Am. Chem. Soc.* **1990**, *112*, 1854–1860.
(38) Anderegg, G.; Räber, M. Metal Complex Formation of a New Siderophore Desferrithiocin and of Three Related Ligands. *J. Chem. Soc., Chem. Commun.* **1990**, 1194–1196.
(39) Bergeron, R. J.; Wiegand, J.; Dionis, J. B.; Egli-Karmakka, M.; Frei, J.; Huxley-Tencer, A.; Peter, H. H. Evaluation of Desferrithiocin and Its Synthetic Analogues as Orally Effective Iron Chelators. *J. Med. Chem.* **1991**, *34*, 2072–2078.
(40) Bergeron, R. J.; Streiff, R. R.; Wiegand, J.; Vinson, J. R. T.; Luchetta, G.; Evans, K. M.; Peter, H.; Jenny, H.-B. A Comparative Evaluation of Iron Clearance Models. *Ann. N. Y. Acad. Sci.* **1990**, *612*, 378–393.
(41) Bergeron, R. J.; Streiff, R. R.; Creary, E. A.; Daniels, R. D., Jr.; King, W.; Luchetta, G.; Wiegand, J.; Moerker, T.; Peter, H. H. A Comparative Study of the Iron-Clearing Properties of Desferrithiocin Analogues with Desferrioxamine B in a *Cebus* Monkey Model. *Blood* **1993**, *81*, 2166–2173.
(42) Bergeron, R. J.; Wiegand, J.; McManis, J. S.; McCosar, B. H.; Weimar, W. R.; Brittenham, G. M.; Smith, R. E. Effects of C-4 Stereochemistry and C-4′ Hydroxylation on the Iron Clearing Efficiency and Toxicity of Desferrithiocin Analogues. *J. Med. Chem.* **1999**, *42*, 2432–2440.
(43) Bergeron, R. J.; Wiegand, J.; McManis, J. S.; Bussenius, J.; Smith, R. E.; Weimar, W. R. Methoxylation of Desazadesferrithiocin Analogues: Enhanced Iron Clearing Efficiency. *J. Med. Chem.* **2003**, *46*, 1470–1477.
(44) Bergeron, R. J.; Wiegand, J.; Weimar, W. R.; Vinson, J. R. T.; Bussenius, J.; Yao, G. W.; McManis, J. S. Desazadesmethyldesferrithiocin Analogues as Orally Effective Iron Chelators. *J. Med. Chem.* **1999**, *42*, 95–108.
(45) Bergeron, R. J.; Wiegand, J.; McManis, J. S.; Bharti, N. The Design, Synthesis, and Evaluation of Organ-Specific Iron Chelators. *J. Med. Chem.* **2006**, *49*, 7032–7043.
(46) Bergeron, R. J.; Wiegand, J.; Bharti, N.; Singh, S.; Rocca, J. R. Impact of the 3,6,9-Trioxadecyloxy Group on Desazadesferrithiocin Analogue Iron Clearance and Organ Distribution. *J. Med. Chem.* **2007**, *50*, 3302–3313.
(47) Bergeron, R. J.; Wiegand, J.; McManis, J. S.; Bharti, N.; Singh, S. Design, Synthesis, and Testing of Non-Nephrotoxic Desazadesferrithiocin Polyether Analogues. *J. Med. Chem.* **2008**, *51*, 3913–3923.
(48) Bergeron, R. J.; Bharti, N.; Wiegand, J.; McManis, J. S.; Yao, H.; Prokai, L. Polyamine Vectored Iron Chelators: The Role of Charge. *J. Med. Chem.* **2005**, *48*, 4120–4137.
(49) Brunner, H; Gruber, N. Carboplatin-Containing Porphyrin−Platinum Complexes as Cytotoxic and Phototoxic Antitumor Agents. *Inorg. Chim. Acta* **2004**, *357*, 4423–4451.
(50) Kitto, H. J.; Schwartz, E.; Nijemeisland, M.; Koepf, M.; Cornelissen, J. J. L. M.; Rowan, A. E.; Nolte, R. J. M. Post-Modification of Helical Dipeptido Polyisocyanides Using the 'Click' Reaction. *J. Mater. Chem.* **2008**, *18*, 5615–5624.
(51) Bergeron, R. J.; Wiegand, J.; Weimar, W. R.; McManis, J. S.; Smith, R. E.; Abboud, K. A. Iron Chelation Promoted by Desazadesferrithiocin Analogues: An Enantioselective Barrier. *Chirality* **2003**, *15*, 593–599.
(52) Sangster, J. *Octanol−Water Partition Coefficients: Fundamentals and Physical Chemistry*; John Wiley and Sons: West Sussex, England, 1997; Vol. 2.
(53) White, G. P.; Jacobs, A.; Grady, R. W.; Cerami, A. The Effect of Chelating Agents on Iron Mobilization in Chang Cell Cultures. *Blood* **1976**, *48*, 923–929.
(54) White, G. P.; Bailey-Wood, R.; Jacobs, A. The Effect of Chelating Agents on Cellular Iron Metabolism. *Clin. Sci. Mol. Med.* **1976**, *50*, 145–52.
(55) Bergeron, R. J.; McManis, J. S.; Weimar, W. R.; Wiegand, J. Eiler-McManis, E. Iron Chelators and Therapeutic Uses. In: Abraham D. A., editor. *Burger's Medicinal Chemistry*, 6th ed.; Wiley: New York: 2003; pp 479−561.
(56) *Torpac Rat and Guinea Pig Capsule and Accessory Pricing*; Torpac: Fairfield, NJ; http://www.torpac.com/Torpac%20Rat%20Gpig%20Pricing.pdf.
(57) *SHELXTL6*; Bruker-AXS: Madison, WI, **2000**.
(58) Bergeron, R. J.; Wiegand, J.; Ratliff-Thompson, K.; Weimar, W. R. The Origin of the Differences in (*R*)- and (*S*)-Desmethyldesferrithiocin: Iron-Clearing Properties. *Ann. N. Y. Acad. Sci.* **1998**, *850*, 202–216.
(59) Bergeron, R. J.; Streiff, R. R.; Wiegand, J.; Luchetta, G.; Creary, E. A.; Peter, H. H. A Comparison of the Iron-Clearing Properties of 1,2-Dimethyl-3-Hydroxypyrid-4-one, 1,2-Diethyl-3-Hydroxypyrid-4-one, and Deferoxamine. *Blood* **1992**, *79*, 1882–1890.
(60) Wood, J. K.; Milner, P. F.; Pathak, U. N. The Metabolism of Iron-Dextran Given As a Total-Dose Infusion to Iron Deficient Jamaican Subjects. *Br. J. Haematol.* **1968**, *14*, 119–129.
(61) Bergeron, R. J.; Wiegand, J.; Brittenham, G. M. HBED: A Potential Alternative to Deferoxamine for Iron-Chelating Therapy. *Blood* **1998**, *91*, 1446–1452.
(62) Bergeron, R. J.; Wiegand, J.; Wollenweber, M.; McManis, J. S.; Algee, S. E.; Ratliff-Thompson, K. Synthesis and Biological Evaluation of Naphthyldesferrithiocin Iron Chelators. *J. Med. Chem.* **1996**, *39*, 1575–1581.